Proper Orthogonal Decomposition and Radial Basis Functions Algorithm for Diagnostic Procedure Based on Inverse Analysis

Vladimir Buljak
Researcher
Politecnico di Milano

Identification procedures based on instrumented indentation and inverse analysis are traditionally coupled with Finite Element Modelling (FEM) to perform simulation of the test. However, this approach is not suitable for in-situ applications since it is rather time consuming due to material and geometrical nonlinearities required to be taken into account. This paper presents a novel technique for system response prediction based on Proper Orthogonal Decomposition and Radial Basis Functions. The developed technique gives the results of the same accuracy as those computed by FEM in computing times shorter by several orders of magnitude. Presented examples consider two different engineering applications. The first deals with the assessment of material parameters entering into the constitutive models of possibly damaged materials used for industrial plants. The second considers the identification of residual stresses which arise in components after surface treatments.

Keywords: *instrumented indentation, inverse analyses, proper orthogonal decomposition, material characterization.*

1. INTRODUCTION

Numerical simulations have been established as a powerful tool used in practically all fields of engineering and science. A large number of commercial codes are developed to solve the so-called *direct problems*, which consist of finding the solution in terms of response fields when a complete set of input data defining uniquely the system is known. Since these codes require the knowledge of some parameters on which the solution depends, sometimes in engineering practice it is required to solve an *inverse problem*, defined as the one where some of the "effects" (responses) are known but not some of the "causes" leading to them, namely the parameters on which the system depends. These problems are tackled within, a relatively young and still growing scientific branch which in the modern literature (e.g. [1]) is found under the name of *Inverse Analyses*.

Inverse analyses are combining experimental mechanics with numerical simulations and mathematical programming. In the first phase of these procedures a test is performed from which some measurable quantities are collected. In the subsequent phase, the same test is simulated. Then, mathematical programming is used to minimize the objective function, which quantifies the discrepancy between measured quantities and their computed counterparts as a function of sought parameters. The solution of the inverse problem is a set of parameters for which the discrepancy between the measured results and those simulated is having its minimum.

Received: May 2010, Accepted: July 2010
Correspondence to: Dr Vladimir Buljak
Politecnico di Milano,
Piazza Leonardo da Vinci 32, 20100 Milano, Italy
E-mail: buljak@stru.polimi.it

In the last decade, approximately, the traditional *hardness testing* has been developed into a methodology of instrumented indentation apt to identify parameters which are needed for reliable computational analysis of structures and industrial products. In the instrumented indentation the process is performed quasi-statically, with constant monitoring of the applied force and resulting penetration. The result of this test is a so-called indentation curve (Fig. 1). Several authors (see e.g. [2-4]) have proposed some semi-empirical approaches to correlate the data provided by indentation curves with Young's modulus and yield stress of the material.

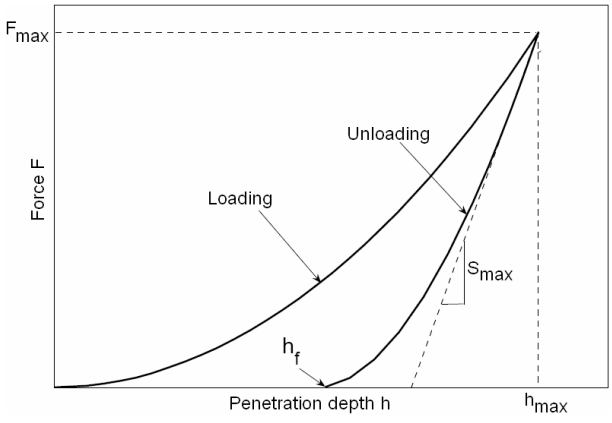

Figure 1. Indentation curve

The use of this experimental technique in the context of inverse analyses brought further improvements. Simulating the indentation test by a commercial finite element code it is possible to reproduce results of high accuracy. Combining these numerical results with those obtained from the experiments within inverse analysis procedure showed that material parameters can be assessed more accurately and in larger numbers. A number of such examples can be found in the literature (e.g. application on

functionally graded materials [5]; on thin films [6]; in [7] the exploitation of both indentation curve and residual imprint was proposed; the same method is successfully applied in [8] to assess residual stresses resulting from surface treatments; in [9] to assess anisotropic material properties, or quasi-brittle fracture properties in [10]).

Inverse analyses based on instrumented indentation tests are recently becoming more and more interesting for diagnostic procedures of components in service. This is due to the fact that, at first, the indentation test is considered to be non-destructive since the volume of material involved in the test is quite small and residual depths that are left behind after the removal of the indenter are usually about 100 μm. In addition, indentation test can be performed completely in-situ on a working component.

In order to have an operable diagnostic procedure completely executable in-situ, apart from portable instrumentation it is also required to have a fast computing tool to solve the inverse problem. Traditional approaches that are based on FE simulations are not suitable for the task, since due to non-linearities present in the model, computing times are elevated, and combined with repetitive computations required by the optimization algorithms, the whole identification process takes hours or even days in some cases. This paper shows a novel methodology based on Proper Orthogonal Decomposition (POD), by which the identification procedure becomes much faster, more economical and robust. The developed approach is bringing inverse analyses to a routine level by decreasing the computing time by several orders of magnitude.

2. ON OPTIMIZATION ALGORITHMS

Within the inverse analyses procedure the discrepancy function is constructed to quantify the difference between experimentally measured results and their computed counterparts from the numerical model that simulates the test. In a subsequent step this function is minimized with respect to sought parameters. In other words, the goal of this minimization is to find those parameters for which the computed response will match the one measured from the experiment. For this purpose, very effective minimization algorithms are used that are capable to find matching parameters after, sometimes, a surprisingly small number of iterations.

A very popular optimization algorithm is a so-called Trust Region (TR) that belongs to a group of first order optimization algorithms. Without entering into the details of how it works, as can be found elsewhere [11,12], the main principles can be outlined as follows.

Let us denote by $\omega(\mathbf{z})$ the discrepancy function that is going to be minimized with respect to sought parameters collected in vector $\mathbf{z}$. In each iteration, k, the quadratic form is constructed to approximate the discrepancy function

$$\omega(\mathbf{z}_k + \mathbf{d}) \approx \omega(\mathbf{z}_k) + \nabla\omega(\mathbf{z}_k)^T(\mathbf{z} - \mathbf{z}_k) + \\ + \frac{1}{2}(\mathbf{z} - \mathbf{z}_k)^T \mathbf{H}(\mathbf{z}_k)(\mathbf{z} - \mathbf{z}_k) = q(\mathbf{z}) \qquad (1)$$

where the Hessian matrix $\mathbf{H}$ is usually approximated to avoid calculation of second derivatives. The next iteration is found by solving for $\mathbf{d}$ that minimizes the constructed quadratic approximation of the objective function. Since this approximation may not be accurate when $\mathbf{z}$ is far from $\mathbf{z}_k$, the search for a minimiser of $q(\mathbf{z})$ is restricted to some region around $\mathbf{z}_k$, called *the trust region* inside which it is trusted that the approximation is fairly good. In practical terms the TR algorithm starts from some guess of sought parameters, then computes the value of discrepancy function and first derivatives with respect to each of the sought parameters collected in vector $\mathbf{z}$. Based on these computations, the next iteration defined by $\mathbf{z}_k + \mathbf{d}$ is computed and the process is iteratively repeated until convergence criteria are met.

The many multiple derivatives approximated by finite difference imply a sequel of direct analyses (namely of response computations based on a sequel of parameter vectors) and, hence, would require heavy computing times if carried out by FE test simulations. Clearly, these optimization algorithms involve in each iteration n + 1 simulations, where n is the number of parameters to be identified.

Even though TR algorithm is a relatively powerful tool for the optimization and usually converges to a solution after about ten iterations, it is not that effective if the objective function to be minimized is strongly non-convex, characterized by a big number of local minima. The TR algorithm cannot distinguish between local and global minima, and will treat as a solution of the optimization problem all mathematical minima (those for which the first derivatives are equal to zero) within the range of optimization.

The alternative to the first order algorithms, capable to overcome the problem of local minima are so-called Genetic Algorithms (GA). The GA represents an optimization tool based on constant modification of "population". At each step, a GA randomly selects individuals from the current population to be "parents" and produce "children" for the next generation. Over successive generations, the population "evolves" toward an optimal solution. The detailed description on GA can be found in other references [13,14]. In what follows is just a brief description of GA together with how they were applied in the present context.

In the context of employing GA to minimize the discrepancy function for diagnostic analyses, each member of the population represents a different combination of sought parameters collected in vector $\mathbf{z}_i$. The so-called "fitness function" that is used to distinguish different members here represents a scalar value of the discrepancy function. In the present context, the discrepancy function represents some norm of a difference between measured quantities and their computed counterparts, like

$$\omega(\mathbf{z}_i) = \mathbf{R}^T \cdot \mathbf{R}\,, \quad \mathbf{R} = \mathbf{Y}_{\mathrm{EXP}} - \mathbf{Y}_{\mathrm{COM}} \qquad (2)$$

where it is assumed that measurable quantities are collected in vector $\mathbf{Y}_{\mathrm{EXP}}$ and their computed counterparts in vector $\mathbf{Y}_{\mathrm{COM}}$.

Optimization by GA proceeds according to following steps:

- At the beginning, the algorithm generates a random set of individuals, let us say M of them, in this case different parameter combinations are collected in vectors $\mathbf{z}_i$, where $i = 1,\ldots, M$.
- In the second step, for each individual from the initial population a discrepancy function is

computed. This implies that for all M members, a simulation of the experiment needs to be performed. Subsequently, all members are sorted based on their value of the fitness function.

- The new generation is created from the individuals contained in the current population by forming the following three groups: "elite kids", "crossover kids" and "mutation kids". "Elite kids" are taken as 2 – 5 % of all individuals with the best value of fitness function and are passed directly to the next generation. A certain number of remaining individuals are selected as parents to form crossover kids. The crossover is performed by the combination of "genes" (in this case parameter values) of two previously selected parents. The remaining group of individuals is created with the process called "mutation" by applying random changes to parameter vectors of individuals with the worst fitness function.

With this procedure the new generation is formed and the old one is replaced by it. The process iteratively continues until convergence criteria are met. The solution of the minimization problem at the end is taken to be the best individual in the last generation.

The main advantage of GA with respect to classical optimization algorithms (like TR) is found in the capability to find the global minimum. This nice feature, however, comes with a price of increased computational time. In the structural problems here presented, it turns out that the usual number of members of the population is equal to 50, while to reach the successful convergence it is required to have more or less 100 generations. This means that the total number of simulations is about 5000.

Comparing it to the first order algorithms, the difference is quite evident. To assess, for instance, three parameters with TR algorithm in each iteration, it will be required to perform 4 (3 + 1) simulations. This number is further multiplied by the number of iterations. Even if the optimization is performed at different times (say 3 or 4) starting from different initializations to confirm that the solution really represents global minimum, still the total number of simulations is about 150 which is one order of magnitude smaller than with GA. Therefore, this implies that it is computationally justifiable to use GA as the optimization tool only in those cases characterized by the discrepancy function with a large number of local minima.

Coupling FE simulations with any optimization algorithm when it is desired to have a fast and robust procedure executable in-situ on "small" computers is not suitable due to elevated computing times. For instance, when the indentation test is used, one simulation approximately takes about 5 minutes (for a simple 2D case). It is therefore evident that even when TR is used, the computing time would be more than 10 hours.

In the following section an alternative formulation will be presented with which practically the same results as those coming from FE simulations are obtained but for computing times shorter by even 5 orders of magnitude. This circumstance makes the identification process extremely fast and robust. Further, it also allows for employing computationally more expensive GA in those situations where they are highly desirable.

3. POD-RBF APPROXIMATION FOR FAST APPROXIMATION OF SYSTEM RESPONSE

Proper Orthogonal Decomposition (POD) is a powerful method of data analysis aimed at obtaining low-dimensional approximate description of some high dimensional processes. Probably the best way to explain what POD is would be on a set of two dimensional vectors.

Let us assume that we would like to construct one dimensional approximation of a set of almost parallel vectors (in POD jargon called closely "correlated" vectors) shown in Figure 2. Obviously, doing that in the original coordinate system will introduce a significant error since both components have the same order of magnitude. On the other hand, we can introduce a new coordinate system with axes rotated by approximately 45° and perform this one-component approximation in the new system. Here the approximation is more accurate since the components to be neglected are for all of the vectors much smaller than the other ones. Finally, if we choose the new coordinate system in such way that the x' axis will have a direction with respect to which the summation of projections of all the vectors from the set is giving the maximum, then we can say that in this basis the best possible (the most accurate) one-component approximation of the given set of vectors is obtained. In such case, the new coordinate basis represents a POD basis for the set of vectors.

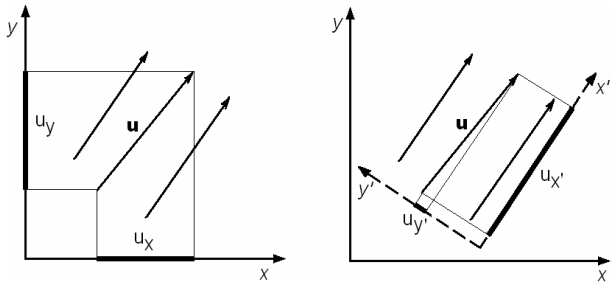

Figure 2. Closely correlated vectors and their projections in the original and new coordinate system

To connect this geometrical interpretation with structural analysis, let us introduce a concept of "snapshots" which is a fundamental notion of POD analyses. In POD jargon, a snapshot represents a collection of N measurements u_i of a certain state variable. In other words, one snapshot is one output of the system that corresponds to a certain input, defined with some parameters on which the system depends. In structural context, of interest here, the system can be represented by a numerical model and the snapshots can be any discrete values of fields of interest, like nodal displacements, values of stresses at integration points, velocities, temperatures, etc. On the other hand, parameters on which the system depends, are taken here to be those that are later going to be identified within inverse analyses.

The collection of M snapshots, generated by changing these parameters, can be stored in rectangular N by M matrix **U**, called the *snapshot matrix*.

The snapshot matrix **U** can be interpreted as a set of M, N-dimensional vectors. Applying the same logic as the one previously presented for two-dimensional vectors, the POD basis for the snapshot matrix **U** can be constructed in the following steps:

- Find the direction with respect to which the summation of projections of all the snapshots attains maximum.
- Find the direction orthogonal to the previous. Of all possible choices, pick up the one that is giving the maximum projection of all the snapshots.
- Find the direction orthogonal to all previously found, having the same optimal property (maximal projection).
- Repeat previous step until the last direction is found.

It can be shown that this maximization process is connected with the auxiliary eigenvalue problem within a process called Principal Component Analyses [15,16]. To construct POD basis of snapshot matrix with this process, one needs to compute eigenvalues (λ_i) and eigenvectors ($\mathbf{v}^i$) of the matrix $\mathbf{D} = \mathbf{U}^T \cdot \mathbf{U}$. After the eigenvalue problem is solved, the generic formula for i-th POD direction is given by

$$\boldsymbol{\varphi}^i = \mathbf{U} \cdot \mathbf{v}^i \cdot \lambda_i^{-\frac{1}{2}} . \tag{3}$$

Then the POD basis represents the $N \times M$ matrix

$$\boldsymbol{\Phi} = \left[\boldsymbol{\varphi}^i \right] \tag{4}$$

where previously computed POD directions are sorted in descending order of corresponding eigenvalues.

Now it is possible to express all the snapshots in the new basis by a linear transformation

$$\mathbf{U} = \boldsymbol{\Phi} \cdot \mathbf{A} \tag{5}$$

where **A** represents "amplitude" matrix that, having in mind the orthogonality of the new basis, $\boldsymbol{\Phi}^T \cdot \boldsymbol{\Phi} = \mathbf{I}$, can be directly computed from

$$\mathbf{A} = \boldsymbol{\Phi}^T \cdot \mathbf{U} . \tag{6}$$

Transformation (5) gives the snapshot matrix in the new coordinate basis. At this stage no approximation is introduced, just the basis is changed. Having in mind the optimal feature of the new basis (i.e. the first direction gives the best possible one component approximation, the first two – the best possible two term, etc.) now it is easy to construct a low-order approximation by keeping the first couple of directions. Performing truncation based on a desired accuracy, by keeping the first P directions, a low-order approximation of the snapshot matrix is given by

$$\mathbf{U} \approx \bar{\boldsymbol{\Phi}} \cdot \bar{\mathbf{A}} \tag{7}$$

where terms with a bar represent truncated matrices. In the same manner, approximation of any single response of the system is given by multiplying the truncated POD basis with corresponding vector of amplitudes

$$\mathbf{u}_i \approx \bar{\boldsymbol{\Phi}} \cdot \bar{\mathbf{a}}_i . \tag{8}$$

The last equation gives an approximate response only for a finite number of cases that were generated in the original snapshot matrix. To pass from this type of a response to a rather continuous one, additional modification needs to be implemented, that defines amplitudes entering into vector $\bar{\mathbf{a}}_i$ not as constants but as some nonlinear functions of parameters on which the system depends. It is done by assuming that each of the entries of the amplitude vector can be written as a linear combination of some non-linear functions of parameters in the following form

$$\bar{a}_k(\mathbf{z}) = \sum_{i=1}^{M} b_k^i \cdot g_i(\mathbf{z}) \tag{9}$$

or, written in the vector form it yields

$$\hat{\mathbf{a}}(\mathbf{z}) = \mathbf{B} \cdot \mathbf{g}(\mathbf{z}) \tag{10}$$

where matrix **B** collects all interpolation coefficients.

The choice of functions g_i is arbitrary and in this study they are chosen to be Radial Basis Function (RBF) [17], defined as a function of some norm between argument of the function and a fixed point in parameter space $g_i(\mathbf{z}) = g_i\left(\left\|\mathbf{z} - \mathbf{z}_i\right\|\right)$. Once the type of RBF is chosen, the only thing that remains is to determine the interpolation coefficients. This is done by writing (10) for all M pairs of parameters $\mathbf{z}_i$ and corresponding responses expressed in new truncated POD basis by $\bar{\mathbf{a}}_i$, and solving for matrix **B**.

Once the interpolation coefficients are determined combining (10) with (8) we arrive to the formulation that is directly giving the approximation of the system response for any arbitrary parameter combination, which reads

$$\mathbf{u}(\mathbf{z}) \approx \bar{\boldsymbol{\Phi}} \cdot \mathbf{B} \cdot \mathbf{g}(\mathbf{z}) . \tag{11}$$

The formulation given by (11), as it will be proved in the examples, gives results practically with the same accuracy as those computed by FE simulation. Obviously the determination of coefficients involves a series of simulations that are time consuming, but done once for all. After this phase, (11) instead of additional simulation, gives practically the same result in about 20000 times shorter computing time, an obvious fact considering that (11) involves a simple matrix multiplication.

4. EXAMPLES OF PARAMETER IDENTIFICATION BY INSTRUMENTED INDENTATION AND POD-RBF FORMULATION

A practical procedure enclosed in small stand-alone software was developed based on two different optimization algorithms: TR algorithm and GA. In both cases the system response, repetitively required by the optimization algorithms was approximated by the POD-RBF formulation, a circumstance that contributed to a huge reduction of overall computing time needed for the identification.

The procedure is calibrated for a conical indentation with the indenter conforming to the standard DS/EN ISO 6508-2. The set of simulations needed to construct matrices later used for determination of coefficients entering into (11) is done using commercial code ABAQUS [18] with an axially-symmetrical mesh visualized in Figure 3.

In this section, results from two different engineering examples are presented. The first considers material characterization in metal plasticity, and the second – assessment of residual stresses resulting from surface treatments.

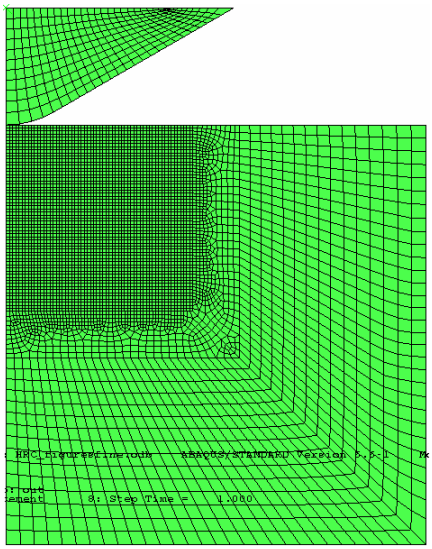

Figure 3. Axially symmetrical mesh used to generate the snapshot matrix

4.1 Material parameter characterization in metal plasticity

This part summarizes some results obtained in a calibration of material parameters of a popular and simple Huber-Mises plasticity material model with exponential hardening. The model is governed by the following parameters: Young's modulus E, yield limit σ_Y, hardening exponent n and Poisson's ratio ν. The procedure was calibrated by keeping a fixed Poisson's ratio equal to 0.3, as this value is not of much interest in diagnostic analyses of metals.

The snapshot matrix was generated varying three material parameters in the following ranges: Young's modulus between 120 and 210 GPa; yield stress between 100 and 400 MPa and hardening exponent between 0.02 and 0.2. The total number of analyses involved equalled 910. Two different snapshot matrices were created, the one for the nodal displacements to be used later for a reconstruction of residual imprint, and the one for the indentation curve. On both snapshot matrices, the previously described POD analysis was performed to create truncated POD basis that is giving a high accuracy, low order approximation. In this particular case, the bases were created by keeping a very small number of directions – for the indentation curve 6, and for the residual imprint – 5 of them. This introduced a huge reduction of the dimensionality of the model without practically any loss of accuracy, since eigenvalues corresponding to kept directions were having 99.99 % of the summation of all of them. This information is directly connected with the low-order approximation accuracy [19], and practically means, that the difference between approximation by (8) differs from the full numerical model (in this case FE simulation) by less than 0.001 %.

The discrepancy function was constructed to give quantitative information of the difference between, both indentation curves and residual imprints. It had a form given by

$$\omega(\mathbf{z}) = \sum_{i=1}^{N_C}\left(\frac{d_i^{\mathbf{COM}} - d_i^{\mathbf{MES}}}{d_{\mathbf{MAX}}}\right)^2 + \sum_{i=1}^{N_I}\left(\frac{u_i^{\mathbf{COM}} - u_i^{\mathbf{MES}}}{u_{\mathbf{MAX}}}\right)^2 . \quad (12)$$

The first part of (12) considers the indentation curve. The total applied load is divided in N_C equal steps (Fig. 4a), and for each of them the corresponding penetration depth d_i was taken both from the experiment (sup MES) and from the model (sup COM). All the differences are normalized with respect to maximal penetration depth obtained at the end of loading step of indentation. The second part quantifies the difference between the two residual imprints, here, due to axial symmetry, represented not by a surface, but with the upper line of the modelled piece that is in contact with the indenter (Fig. 4b). Along this line, N_I heights from the horizontal specimen surface are taken both from the computed model and from the experiment, and the differences are normalized with respect to maximum residual depth u_{MAX} that remains after the indenter is removed.

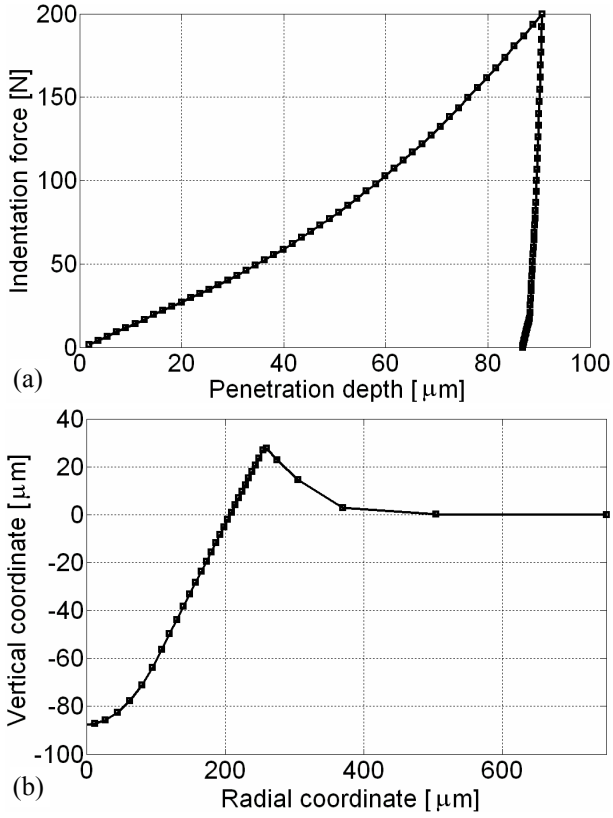

Figure 4. Indentation curve and residual imprint as inputs for the inverse analyses

This discrepancy function is further minimized with respect to three sought parameters that are uniquely defining the stress-strain curve of the indented material.

To test the procedure, first a set of inverse analyses is solved using so-called pseudo-experimental data. These data represent computer generated indentation curves and residual imprints using different combinations of material parameters. The solution of inverse analyses fed by these pseudo-experimental data should equal the parameter values used to generate them, if the inverse problem is well posed.

With the same FE model, additional 50 simulations were performed using only those parameter combinations that were not considered in the generation of the snapshot matrix. The results of these simulations are further used as inputs to the inverse analyses to identify three material parameters. Errors of assessed parameters resulting from each of 50 performed inverse

analyses are visualized in Figure 5. The fact that an average error on identified parameters was about 1 % proved, not only that the inverse problem was well posed, but also the fast formulation proposed in this paper has a so-called generalization feature meaning that it can also accurately reproduce the responses for the inputs not considered in the phase of "training" i.e. the process of generation of snapshot matrix.

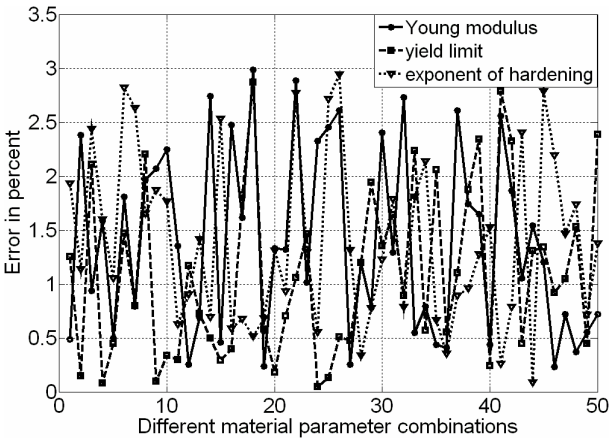

Figure 5. Results of inverse analyses performed on 50 different pseudo-experimental inputs

In the second phase the procedure was verified with real experimental data performed on copper using the instrumented indenter Fischerscope H100, by applying a maximum indentation force equal to 200 N. Results from five different indentation tests were used as inputs to inverse analyses and identified stress-strain curves are visualized in Figure 6. The discrepancy between different curves is very small suggesting that material parameters are assessed with good accuracy. A further check was performed by using identified parameters to simulate the indentation test on a larger scale, with maximum force of 1500 N. The same indentation was performed experimentally, and Figure 7 visualizes the results from the simulation together with experimental data, measured with laser profilometer. It may be observed from the figure that the two profiles practically coincide proving that material parameters were assessed accurately.

4.2 Assessment of the residual stress profile coming from surface treatment

In this section some results considering the assessment of Residual Stresses (RS) resulting from surface treatments are presented. For a more detailed discussion on identification of RS based on instrumented indentation, the reader should refer to [8] and [20]. In the context presented here, the example is interesting since it is characterized by an extremely non-convex discrepancy function and as such, it is practically non-solvable with the TR algorithm.

Applying surface treatments to cylindrical parts creates an axisymmetric RS distribution, usually of the kind visualized in Figure 8 [21,22].

This type of stress distribution is assessed by a presented methodology based on the indentation test. In order to extract information on through-thickness RS distribution in the considered applications, indentation is performed repeatedly under displacement control, up to 3 different depths (to 20, 50 and 150 μm). In this section just some results considering pseudo-experimental data are shown.

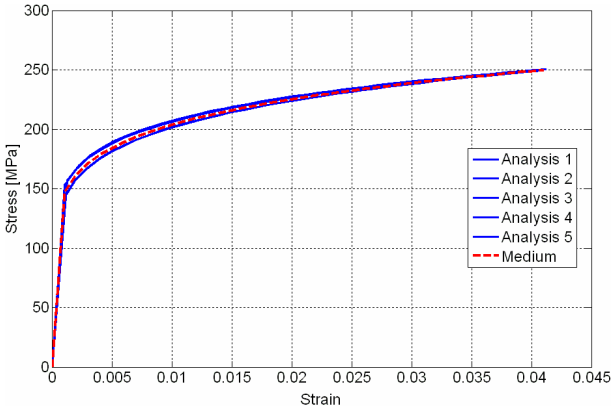

Figure 6. Resulting stress-strain curves identified by inverse analyses from 5 different experiments performed with the same specimen

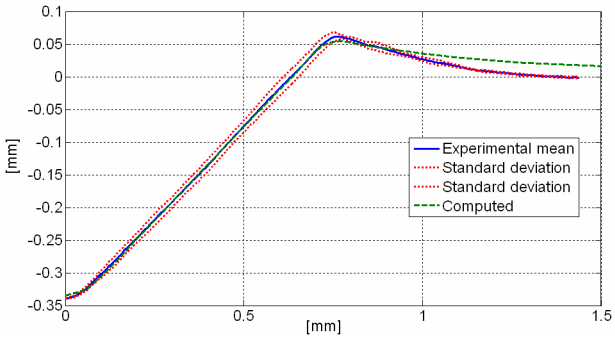

Figure 7. Experimental residual imprint vs. computed one for the indentation with a force of 1500 N

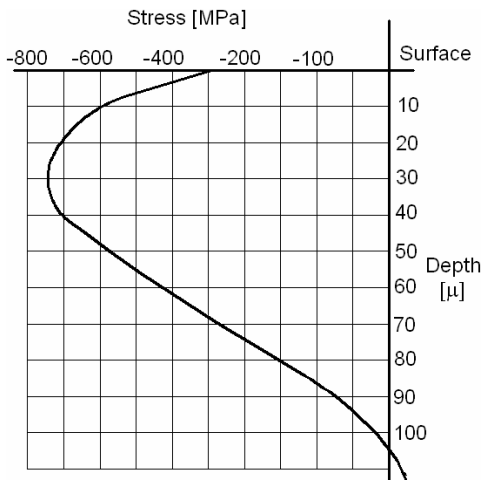

Figure 8. Usual stress distribution after surface treatments

To test the robustness of the procedure, the RS in the considered case were relatively far from yield limit. This is already evidenced in the literature as a more difficult case to analyze [20]. Material parameters used in the simulations were the following: Young's modulus 202 GPa; Poisson's ratio 0.3; yield stress 1060 MPa, while the introduced RS in the model used to generate pseudo-experimental data had a profile visualized in Figure 9, having the maximum value at about 50 % of yield limit.

After pseudo-experimental data were generated, they were used as inputs to the inverse analyses that used POD-RBF formulation "trained" with 768 simulations. The discrepancy function was created in the same way

as the one defined by (12), except that here it had three parts referring to three different indentation tests. First, the inverse problem was solved using TR algorithm. From the results, visualized in Figure 10 it is quite evident that the discrepancy function was characterized with a large number of local minima. This made the problem practically unsolvable with TR since the result turned out to be dependent on the initialization point.

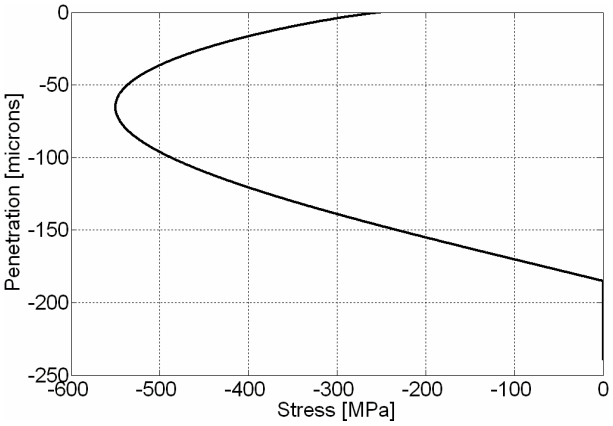

Figure 9. Target distribution of RS to be identified within inverse analyses procedure

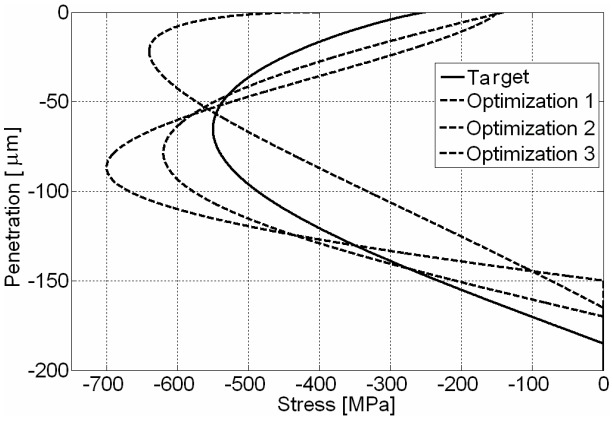

Figure 10. Results of three different optimizations by TR corresponding to different initializations

The same problem was then solved using GA. Figure 11 shows results from four different optimizations. It can be noted that in all the cases, the obtained RS distribution was quite close to the target, confirming the advantage of GA with respect to first order algorithms when the minimization function is characterized by a presence of a large number of local minima.

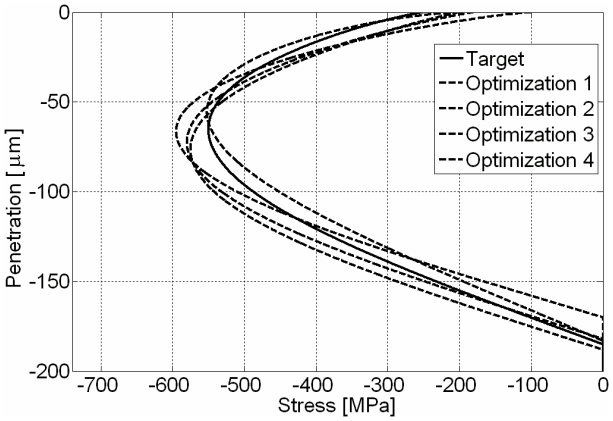

Figure 11. Results of four different optimizations by GA

5. CONCLUDING REMARKS

This paper presented a novel methodology that combines POD with RBF into a fast formulation that can be used to compute system responses in situations in which repetitive simulations are required of the same system by changing just some parameters on which the system depends. This circumstance is frequently encountered in optimization procedures, like diagnostic analyses based on instrumented indentation, discussed here.

Examples treated in this paper show that material parameter characterization becomes more robust and much faster if the developed technique is applied, since the computing times are cut down by several orders of magnitude. Combining the software based on this technique with nowadays existing portable indenters it is possible to create a powerful stand-alone device for in-situ material characterization.

In the second example presented in this paper it is proved that, by having such a fast procedure to compute system response, it is possible to use more "expensive" optimization algorithms, like GA, which in some situations are inevitable. The use of GA in the present context when the test simulation is performed by FEM is possible only theoretically, since one identification process would last for about half a year.

Even though this work is engineeringly motivated by a need of several industrial companies to perform material characterization on working components, it should be mentioned that the developed method is not by any means limited to this purpose only. Today, practically all laboratory-based instrumented indenters have the possibility to evaluate some material parameters usually by using semi-empirical formulae (e.g. Oliver and Pharr [23]). On the other hand, previous works devoted to instrumented indentation, simulation and inverse analysis ([5-9]) showed the possibility to solve more complicated parameter identification problems, but they are more time-consuming and less robust with respect to semi-empirical formulae. Using the once-for-all trained POD-RBF procedure to perform simulations of the indentation test, a simple software can be generated and routinely used in combination with instrumented indenters to assess material parameters in larger numbers and in a more accurate way, since the time needed to assess material properties, when the POD-RBF procedure is used becomes shorter than the time needed to perform the indentation test itself.

ACKNOWLEDGEMENT

The author would like to thank personnel from ENI and Venezia Tecnologie (VeTec) companies for the contribution to this research, coming from a fruitful cooperation between the research team at Politecnico di Milano and these companies.

REFERENCES

[1] Groetsch, C.W.: *Inverse Problems: Activities for Undergraduates*, The Mathematical Association of America, Washington, D.C., 1999.

[2] Jäger, A., Lackner, R. and Eberhardsteiner, J.: Identification of viscoelastic properties by means of

nanoindentation taking the real tip geometry into account, Meccanica, Vol. 42, No. 3, pp. 293-306, 2007.

[3] Nix, W.D. and Gao, H.: Indentation size effects in crystalline materials: A law for strain gradient plasticity, Journal of the Mechanics and Physics of Solids, Vol. 46, No. 3, pp. 411-425, 1998.

[4] Pharr, G.M.: Measurement of mechanical properties by ultra-low load indentation, Materials Science and Engineering A, Vol. 253, No. 1-2, pp. 151-159, 1998.

[5] Nakamura, T., Wang, T. and Sampath, S.: Determination of properties of graded materials by inverse analysis and instrumented indentation, Acta Materialia, Vol. 48, No. 17, pp. 4293-4306, 2000.

[6] Van Vliet, K.J. and Gouldstone, A.: Mechanical properties of thin films quantified via instrumented indentation, Surface Engineering, Vol. 17, No. 2, pp. 140-145, 2001.

[7] Bolzon, G., Maier, G. and Panico, M.: Material model calibration by indentation, imprint mapping and inverse analysis, International Journal of Solids and Structures, Vol. 41, No. 11-12, pp. 2957-2975, 2004.

[8] Bolzon, G. and Buljak, V.: An indentation-based technique to determine in-depth residual stress profiles induced by surface treatment of metal components, Fatigue & Fracture of Engineering Materials & Structures, accepted for publication.

[9] Bocciarelli, M., Bolzon, G. and Maier, G.: Parameter identification in anisotropic elastoplasticity by indentation and imprint mapping, Mechanics of Materials, Vol. 37, No. 8, pp. 855-868, 2005.

[10] Maier, G., Bocciarelli, M., Bolzon, G. and Fedele, R.: Inverse analyses in fracture mechanics, International Journal of Fracture, Vol. 138, No. 1-4, pp. 47-73, 2006.

[11] Nocedal, J. and Wright, S.J.: *Numerical Optimization*, Springer-Verlag, New York, 2006.

[12] *Optimization Toolbox 3 – User's Guide*, The MathWorks, Inc., Natick, 2006.

[13] *Generic Algorithms and Direct Search Toolbox 2 – User's Guide*, The MathWorks, Inc., Natick, 2006.

[14] Goldberg, D.E.: *Genetic Algorithms in Search, Optimization and Machine Learning*, Addison-Wesley, Reading, Massachusetts, 1989.

[15] Liang, Y.C., Lee, H.P., Lim S.P., Lin, W.Z., Lee, K.H. and Wu, C.G.: Proper orthogonal decomposition and its applications – part I: Theory, Journal of Sound and Vibration, Vol. 252, No. 3, pp. 527-544, 2002.

[16] Buljak, V.: *Assessment of Material Mechanical Properties and Residual Stresses by Indentation Simulation and "Proper Orthogonal Decomposition"*, PhD thesis, Politecnico di Milano, Milan, 2009.

[17] Buhmann, M.D.: *Radial Basis Functions*, Cambridge University Press, Cambridge, 2003.

[18] *ABAQUS/Standard, Theory and User's Manuals, Release 6.2-1*, HKS Inc., Pawtucket, 1998.

[19] Berkooz, G., Holmes, P. and Lumley, J.L.: The proper orthogonal decomposition in the analysis of turbulent flows, Annual Review of Fluid Mechanics, Vol. 25, pp. 539-575, 1993.

[20] Bocciarelli, M. and Maier, G.: Indentation and imprint mapping method for identification of residual stresses, Computational Materials Science, Vol. 39, No. 2, pp. 381-392, 2007.

[21] McClung, R.C.: A literature survey on the stability and significance of residual stresses during fatigue, Fatigue & Fracture of Engineering Materials & Structures, Vol. 30, No. 3, pp. 173-205, 2007.

[22] Nalla, R.K., Altenberger, I., Noster, U., Liu, G.Y., Scholtes, B. and Ritchie, R.O.: On the influence of mechanical surface treatments – deep rolling and laser shock peening – on the fatigue behavior of Ti-6Al-4V at ambient and elevated temperatures, Materials Science and Engineering A, Vol. 355, No. 1-2, pp. 216-230, 2003.

[23] Oliver, W.C. and Pharr, G.M.: An improved technique for determining hardness and elastic modulus using load and displacement sensing indentation experiments, Journal of Materials Research, Vol. 7, No. 6, pp. 1564-1583, 1992.

АЛГОРИТАМ БАЗИРАН НА ПРАВИЛНОЈ ОРТОГОНАЛНОЈ ДЕКОМПОЗИЦИЈИ И РАДИЈАЛНИМ БАЗИСНИМ ФУНКЦИЈАМА ЗА ПРОЦЕДУРЕ У ДИЈАГНОСТИЦИ НА БАЗИ ИНВЕРЗНЕ АНАЛИЗЕ

Владимир Буљак

Процедуре карактеризације материјала базиране на тестовима инструментираног утискивања и инверзним анализама, традиционално користе Методу коначних елемената (МКЕ) за симулирање теста. Тај приступ међутим није адекватан за примене на терену, обзиром да ове симулације трају релативно дуго као последица нелинеарности присутних у моделу. Овај рад представља нови приступ предвиђања одговора система базиран на Правилној ортогоналној декомпозицији (*Proper Orthogonal Decomposition*) и Радијалним базисним функцијама (*Radial Basis Functions*). Развијена техника даје резултате на истом нивоу тачности као и МКЕ, за време краће за 4 до 5 реда величине. Приказани примери третирају две различите инжењерске примене. Прва се односи на карактеризацију металних, потенцијално оштећених, материјала од којих су израђене различите индустријске компоненте у активној употреби. Други пример разматра идентификацију заосталих напона који се јављају као последица различитих површинских обрада.